Proceedings of the ASME 2016 35th International Conference on Ocean, Offshore and Arctic Engineering
OMAE2016
June 19-24, 2016, Busan, South Korea

OMAE2016-54994

A 3D HIGHER ORDER TIME DOMAIN RANKINE PANEL METHOD FOR WAVE-CURRENT INTERACTION

Felipe Ruggeri
Numerical Offshore Tank (TPN)
University of São Paulo
São Paulo, Brazil
Email: felipe.ruggeri@usp.br

Rafael A. Watai
Argonautica Engineering & Research
São Paulo, Brazil
Email: watai@argonautica.com.br

Alexandre N. Simos
Numerical Offshore Tank (TPN)
University of São Paulo
São Paulo, Brazil
Email: alesimos@usp.br

ABSTRACT

The wave-current effects are very important in several offshore applications, for instance, the wave-drift-damping of a Turret moored FPSO. This papers presents the incorporation of current effects in the higher order time domain Rankine Panel Method on development in the Numerical Offshore Tank (TPN) at the University of São Paulo (USP) already introduced in [1]. The method is based on a perturbation theory to study first and second order effects, considering the geometry described using NURBS (Non Uniform Rational Basis Spline) and the potential function, free surface elevation, pressure etc by B-splines of arbitrary degree. The study is performed for a simplified geometry (sphere) and the results regarding a fixed hemisphere compared to other numerical methods considering both first and second order quantities are presented.

KEYWORDS

Time domain Rankine Panel Method, Seakeeping, Wave-current interaction.

INTRODUCTION

The prediction of body forces/motions are important in several practical applications, where design/operational conditions should be defined. The wave-current interaction can change the zero current solution appreciably, which is investigated using an extension of the higher order time domain rankine panel method introduced in [1], where the potential function, free surface elevation are described using a B-spline approach and the body geometry using a NURBS description [2].

The methodology developed by the Numerical Offshore Tank (TPN) is the pre-analysis of the most critical conditions by numerical simulations, validation of the numerical estimations with experimental data and then extrapolation to real scale concerning all conditions. This paper describes the inclusion of current effects in a code based on Rankine sources on time domain for the prediction of platform motions using a higher order approach, which has started in a 2D version [3] and lately extended to a 3D lower order version [4].

However the computation of mean drift forces, slow drift forces and wave-current interaction required the computation of the derivatives of the velocity potential. These facts motivated the development of a higher order approach in the numerical method since the quantities in the panel following a low order approach are constant in each panel, therefore the prediction of the velocity field is poor, as the wave runup close to the body. The limitations of a constant panel method are presented, for instance, in [5] and some comparisons regarding the accuracy and computational time of both approaches can be seen in [6]. Several commercial/academic codes have been developed in the last years for wave-structure interactions, see for instance, SeaFEM [7], WAMIT [8], AQWA [9], THOBEM considering quadratic quadrilateral elements (8 nodes) [6], the 9-node quadratic elements from [10], the 12-node cubic elements from [11], as the B-splines from [12] (included in the higher order module of WAMIT), the last one following a frequency domain approach without current effects.

The accurate spatial derivatives computation is particularly important for the so-called "m-terms" evaluation, introduced by [13] and studied by several authors, see for instance [14] and [15], that are required for free floating simulations. In this paper only results for fixed structures are presented since it is the first step in the validation procedure of wave-current computations, therefore the "m-terms" are not presented. However, since the next step is the free floating simulations, the formulation is presented in time domain considering a generic case including fixed, prescribed motions and free floating structures.

The time domain approach is chosen due to the possibility of inclusion of both weak and strong non-linearities in the hydrodynamic problem, which can be performed simpler in time domain formulation compared to the traditional frequency domain approach. This method usually computes the hydrodynamic coefficients (added mass, wave damping, diffraction force etc.) using the wave source Green function from [16] to avoid free surface discretization and after the solution is simulated in time-domain using Cummins equation [17].

It should be noticed that some important non-linear effects are verified for the wave drift damping regarding the yaw equilibrium of a ship shape turret platform, as the wave runup about a cylindrical and cone shaped foundations for offshore wind turbines, that change appreciably under current effects.

MATHEMATICAL PROBLEM

The mathematical problem is described as a collection of floating and fixed structures under the incidence of waves and current. The flow is assumed as irrotational and the fluid as ideal with the free surface assumed as a mathematical function. The weakly non-linear approach is applied assuming all quantities as describes by Stokes series, see for instance Eqn. 1, which are replaced in the traditional no flux condition for fixed and floating bodies and in the kinematic and dynamic free surface conditions.

$$\varphi = \varphi^{(0)} + \sum_{i=1}^{\infty} \varphi^{(i)}(t).\varepsilon^i \tag{1}$$

The zero order potential is decomposed in the incident current field (Ux) and the disturbance zero order potential ($\phi_S^{(0)}$), Eq. 2. The BVP is stated from Eqn. 3 to 6, assuming the double-body linearization, there $\bar{S}_{fs}$ is the mean free surface level outside the body, $\bar{S}_{fixed}$, $\bar{S}_{pm}$ and $\bar{S}_{fb}$ are the mean submerged surfaces of fixed bodies, prescribed motion and floating bodies with $\vec{n}$ normal vector (n_x, n_y and n_z components).

$$\varphi^{(0)} = \phi_S^{(0)} + Ux \tag{2}$$

$$\nabla^2 \phi_S^{(0)} = 0, \ in\ \bar{\Omega} \tag{3}$$

$$\frac{\partial \phi_S^{(0)}}{\partial z} = 0, \ in\ Q \in \bar{S}_{fs} \tag{4}$$

$$\frac{\partial \phi_S^{(0)}}{\partial n} = -Un_{xQ}, \ in\ Q \in \bar{S}_{fixed} \cup \bar{S}_{pm} \cup \bar{S}_{fb} \tag{5}$$

$$\nabla \phi_S^{(0)} \to \vec{0}, |\vec{x}| \to \infty \tag{6}$$

The first order problem concerning both the velocity and acceleration potential coupled to motion equations can be summarized from Eqn. 10 to 16, already replacing the first order potential decomposition shown in Eqn. 7. The "mixed" zero/first order potential terms are also present in these conditions, where $\phi_s^{(1)}$ is the disturbance first order potential, that takes into account all hydrodynamic effects (i.e: radiation, diffraction etc.) while $\phi_I^{(1)}$ is the first order incident wave field assuming the superposition of several regular components with amplitude A_i, g the gravity acceleration module, k_i the wave number, β_i the wave direction (measured from the axis x in the counter-clockwise), δ_i the relative phase, ω_{i0} the wave frequency and ω_i the encounter frequency, assuming the correction shown in Eqn. 9. The free surface conditions shown in Eqn 11 and 12 contain additional terms to absorb the radiated/diffracted waves following a "sponge layer" approach introduced by [18] and discussed in more details in [4].

The terms $[M]$, $[C^{(0)}]$ and $[K^{(0)}]$ in Eqn. 16 are the mass, external damping and total stiffness matrix (hydrostatic+external). The acceleration potential approach is assumed to provide stability in the time domain simulation, as discussed by [19], [20] and [21].

The first order body motions are defined by $\{X^{(1)}\}$, the velocity of the center of gravity by $\vec{v_G}$ in the translational DoF and $\vec{\omega}$ for the rotational ones. The vector $\vec{m}_Q$ contain the so-called "m-terms" introduced by [13] and are re-arranged to split the time-variant terms from the constant ones (geometric ones) in order to avoid the re-computation of the terms at each time-step.

$$\varphi^{(1)} = \phi_S^{(1)} + \phi_I^{(1)} \tag{7}$$

$$\phi_I^{(1)} = \sum_{i=1}^{N} \frac{A_i g}{\omega_{i0}} e^{k_i z} \cos(k_i x \cos\beta_i + k_i y \sin\beta_i - \omega_i t + \delta_i) \quad (8)$$

$$\omega_i = |Uk\cos\beta_i - \omega_{i0}| \quad (9)$$

$$\nabla^2\phi_S^{(1)} = 0,\ \nabla^2\Big(\frac{\partial\phi_S^{(1)}}{\partial t}\Big) = 0,\ in\ \bar{\Omega} \quad (10)$$

$$\frac{\partial\phi_S^{(1)}}{\partial t} + g\eta_S^{(1)} + (\frac{\partial\phi_I^{(1)}}{\partial t} + g\eta_I^{(1)}) + \nabla\varphi^{(0)}\cdot\nabla\varphi^{(1)} - \nu\eta_S^{(1)} = 0,\ in\ Q \in \bar{S}_{fs} \quad (11)$$

$$\frac{\partial\eta_S^{(1)}}{\partial t} - \frac{\partial\phi_S^{(1)}}{\partial z} + (\frac{\partial\eta_I^{(1)}}{\partial t} - \frac{\partial\phi_I^{(1)}}{\partial z}) + + \nabla\varphi^{(0)}\cdot\nabla\eta^{(1)} + \frac{\partial^2\varphi^{(0)}}{\partial z^2}\eta^{(1)} - \nu\phi_S^{(1)} = 0,\ in\ Q \in \bar{S}_{fs} \quad (12)$$

$$\frac{\partial\phi_{S_Q}^{(1)}}{\partial n_Q^{(0)}} = -\frac{\partial\phi_{I_Q}^{(1)}}{\partial n_Q^{(0)}}, \quad \frac{\partial^2\phi_{S_Q}^{(1)}}{\partial n_Q^{(0)}\partial t} = -\frac{\partial^2\phi_{I_Q}^{(1)}}{\partial n_Q^{(0)}\partial t},\ \ Q \in \bar{S}_{fixed} \quad (13)$$

$$\frac{\partial\phi_{S_Q}^{(1)}}{\partial n_Q^{(0)}} = [\vec{n}_Q^{(0)}, (Q^{(0)} - G^{(0)}) \wedge \vec{n}_Q^{(0)}]\cdot\{\vec{v}_G^{(1)}, \vec{\omega}^{(1)}\} + \vec{m}_Q \cdot \vec{X^{(1)}},\ Q \in \{\bar{S}_{pm} \cup \bar{S}_{fb}\} \quad (14)$$

$$\frac{\partial^2\phi_{S_Q}^{(1)}}{\partial n_Q^{(0)}\partial t} = [\vec{n}_Q^{(0)}, (Q^{(0)} - G^{(0)}) \wedge \vec{n}_Q^{(0)}]\cdot\{\vec{a}_G^{(1)}, \dot{\vec{\omega}}^{(1)}\} \quad \vec{m}_Q\cdot\{\vec{v}_G^{(1)}, \vec{\omega}^{(1)}\}\ Q \in \{\bar{S}_{pm} \cup \bar{S}_{fb}\} \quad (15)$$

$$[M]\{\ddot{X}^{(1)}\} + [C^{(0)}]\{\dot{X}^{(1)}\} + [K^{(0)}]\{X^{(1)}\} = -\rho\iint_{\bar{S}_{fb}} \Big[\frac{\partial\varphi_Q^{(1)}}{\partial t} + \nabla\varphi_Q^{(0)}\cdot\nabla\varphi_Q^{(1)}\Big]\Big\{ \begin{matrix} \vec{n}_Q^{(0)} \\ (Q^{(0)} - G^{(0)}) \wedge \vec{n}_Q^{(0)} \end{matrix} \Big\} dS_Q \quad (16)$$

The second-order forces considering only the interaction of first order and zero order quantities can be computed using Eqn. 17, where $\vec{\alpha}^{(1)} = (X_4^{(1)}, X_5^{(1)}, X_6^{(1)})$.

$$\vec{F}^{(2)} = -\iint_{\bar{S}_{fb}} \Big(\frac{1}{2}\nabla\varphi_Q^{(1)}\cdot\nabla\varphi_Q^{(1)} + \vec{x}_Q^{(1)}\cdot\nabla\frac{\partial\varphi_Q^{(1)}}{\partial t} + \nabla\varphi_Q^{(0)}\cdot\nabla(\nabla\varphi_Q^{(1)}\cdot\vec{x}_Q^{(1)})\Big)\vec{n}dS - \rho\vec{\alpha}\wedge\iint_{\bar{S}_{fb}}\Big(\frac{\partial\varphi_Q^{(1)}}{\partial t} + \nabla\varphi_Q^{(0)}\cdot\nabla\varphi_Q^{(1)}\Big)\vec{n}dS - \frac{1}{2}\rho g\oint_{WL}[\eta_Q^{(1)} - X_3^{(1)} - \vec{\alpha}^{(1)}\wedge\vec{x}_Q^{(0)}]^2\vec{n}dl \quad (17)$$

The equations and conditions presented so far are enough to guarantee an unique solution to the boundary value problem. The mathematical problem is solved applying Green's identity assuming the Rankine sources as the Green function, leading to Eqn. 18. It should be noticed that in the developed method only points located on continuous region of the surface are considered, therefore the contribution due to the solid angle will be 2π regardless the geometry discretization.

$$\iint_{\partial\bar{\Omega}_{-P}} \Big(\phi_{S_Q}\frac{\partial G_{PQ}}{\partial n_Q} - G_{PQ}\frac{\partial\phi_{S_Q}}{\partial n_Q}\Big)d\partial\Omega_Q = \begin{cases} -4\pi\phi_{S_P},\ if\ P\ is\ \Omega \\ -2\pi\phi_{S_P},\ if\ P\ is\ at\ \partial\Omega \\ 0,\ if\ P\ is\ outside\ \Omega \end{cases} \quad (18)$$

The computational domain considered in Eqn. 18 changes according to the order of the problem (zero/first/second) to improve the convergence rate of the zero order potential. The first order potential is solved considering the computational domain as $\bar{\Omega} = \bar{S}_{fs} \cup \bar{S}_{fixed} \cup \bar{S}_{pm} \cup \bar{S}_{fb}$ and the "simple" Rankine source as Green function (Eqn. 19), while the zero order problem is solved considering the computational domain as $\bar{\Omega} = \bar{S}_{fixed} \cup \bar{S}_{pm} \cup \bar{S}_{fb}$, neglecting the free surface domain and adding the image of the Rankine source about the plane z=0 as Green function (Eqn. 20).

$$G^{(1)} = \frac{1}{r_{PQ}} = \frac{1}{\sqrt{(x_P - x_Q)^2 + (y_P - y_Q)^2 + (z_P - z_Q)^2}} \quad (19)$$

$$G^{(0)} = \frac{1}{r_{PQ}} + \frac{1}{r'_{PQ}} = \frac{1}{\sqrt{(x_P - x_Q)^2 + (y_P - y_Q)^2 + (z_P - z_Q)^2}} + \frac{1}{\sqrt{(x_P - x_Q)^2 + (y_P - y_Q)^2 + (z_P + z_Q)^2}} \quad (20)$$

NUMERICAL METHOD

Geometry

The geometry is described assuming a standard "igs" file, one of the industry standards, which in the context of a panel method contains essentially the surface representation using NURBS. This description is based on the superposition of spline functions properly weighted, which are generically given by Eqn. 21, where p is the basis function degree, u is the point on the curve domain and u_i are the knots vector in the interior region. It should be noticed that the spline of degree p (considering p>0) is defined by a recurrence equation, where the spline of degree 0 is given by Eqn. 22, which is piecewise continuous.

$$N_{i,p}(u) = \frac{u - u_i}{u_{i+p} - u_i} N_{i,p-1}(u) + \frac{u_{i+p+1} - u}{u_{i+p+1} - u_{i+1}} N_{i+1,p-1}(u), \; p > 0 \quad (21)$$

$$N_{i,0}(u) = \begin{cases} 1, \; if \; u_i \leqslant u < u_{i+1} \\ 0, \; if \; u < u_i \; or \; u \geqslant u_{i+1} \end{cases} \quad (22)$$

Since a surface has 2 degrees of freedom, it can be built using 2 orthogonal splines polynomials combined in generic directions u and v to provide the surface domain. Although the surface domain can be generic because the u knots and v knots could be arbitrary, it is convenient to "scale" it into the square of dimensions [0,1]x[0,1] in order to simplify the algebraic manipulations. The i^{th} basis function of degree k are null at all domain but in the range $[u_i, u_{i+k+1}]$, so the basis function have a local influence region, which allows almost any smooth continuous arbitrary function to be represented using NURBS without an excessive computational effort. This characteristic is very useful specially for complex surfaces, such as the stern or a bulb of a ship, since moving the surface control points will not change the entire surface, just a small region surrounding the control point. An example of the combined b-spline curves of degree 2 can be seen in Figure 1, where it is shown the combined $N_2(u)N_2(v)$ function for knot vectors $\{0,0.1,0.2,0.3,0.4,0.5,0.6,0.7,0.8,0.9,1\}$ and is clear that the function has only a localized influence. The NURBS surface is created considering expression 23, where $\vec{C}_{ij}$ are the control points of the surface and w_{ij} are the respective weights.

An example of geometries described using NURBS approach can be seen in Figure 2, concerning simple 1 patch

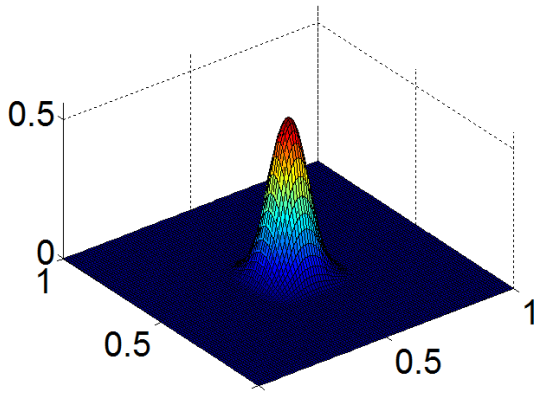

FIGURE 1. Example of shape function.

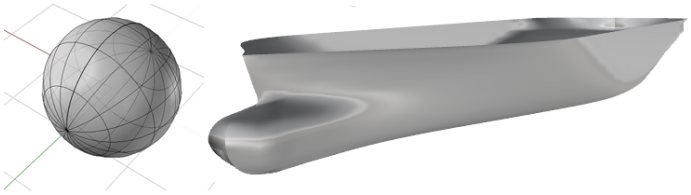

FIGURE 2. Example of geometries described by NURBS (sphere-left and containership - right).

geometries (i.e: sphere) and more complex one (i.e:semi-submersible platform). The normal vector can be computed from the cross product of the position vector in parametric space in both directions (u and v), as shown in Eqn. 24.

$$\begin{Bmatrix} x(u,v) \\ y(u,v) \\ z(u,v) \end{Bmatrix} = \frac{\sum_{i=1}^{N_u} \sum_{j=1}^{N_v} w_{ij} \vec{C}_{ij} N_{i,p}(u) N_{j,p}(v)}{\sum_{i=1}^{N_u} \sum_{j=1}^{N_v} w_{ij} N_{i,p}(u) N_{j,p}(v)}, 0 \leqslant u \leqslant 1, 0 \leqslant v \leqslant 1 \quad (23)$$

$$\vec{n} = \left(\frac{\partial \vec{X}}{\partial u} \wedge \frac{\partial \vec{X}}{\partial v} \right) / \left| \frac{\partial \vec{X}}{\partial u} \wedge \frac{\partial \vec{X}}{\partial v} \right| \Rightarrow \vec{X}(u,v) = (x(u,v), y(u,v), z(u,v)) \quad (24)$$

Potential function and other quantities

The solution quantities (i.e: potential function, velocity field, pressure etc.) are represented using B-spline functions therefore the surface approximation is independent of the solution, which is desirable in the context of a generic method. There is no additional consideration regarding the continuity of the potential function among patches since it would be really difficult from the topology point of view and would require a previous knowledge concerning the flow because on corners the potential

function could be discontinuous due to high gradients (i.e: corners).

However, since the solution is built inside the parametric space of each patch an additional "hidden" layer should be considered to avoid the potential function to be null in the ends of the parametric space.

The disturbance velocity potential (acceleration potential, free surface elevation etc.) are given generically by Eqn. 25, where $\phi_{i,j}^{(n)p}$ are the coefficient corresponding to the i^{th} basis function in direction u, j^{th} basis function in direction v corresponding of the p^{th} patch of the domain considering the nth disturbance velocity potential (first or second order quantities). The basis functions have degree k_u , k_v in the u and v direction, respectively[1].

$$\phi_S^{(n)}(u,v) = \sum_{p=0}^{N_p}\sum_{i=0}^{N_u}\sum_{j=0}^{N_v}\phi_{i,j}^{(n)p}N_i^{k_u,p}(u)N_j^{k_v,p}(v) \tag{25}$$

Potential function derivatives

The potential function first derivatives in the bodies and first order quantities in the free surface can be evaluated by computing the derivative in u and v directions using Eqn. 26 since the shape functions are continuous. However this derivatives are defined in the parametric space, which should be converted to the physical space using Eqn. 27 to provide the velocity field.

$$\begin{aligned}\frac{\partial\varphi}{\partial u}(u,v) &= \sum_{p=0}^{N_p}\sum_{i=0}^{N_u}\sum_{j=0}^{N_v}\phi_{i,j}^{p}\frac{\partial N_i^{k_u,p}(u)}{\partial u}N_j^{k_v,p}(v)\\ \frac{\partial\varphi}{\partial v}(u,v) &= \sum_{p=0}^{N_p}\sum_{i=0}^{N_u}\sum_{j=0}^{N_v}\phi_{i,j}^{p}N_i^{k_u,p}(u)\frac{\partial N_j^{k_v,p}(v)}{\partial v}\end{aligned} \tag{26}$$

$$\left\{\begin{array}{c}\frac{\partial\varphi}{\partial x}\\ \frac{\partial\varphi}{\partial y}\\ \frac{\partial\varphi}{\partial z}\end{array}\right\}_{(x(u,v),y(u,v),z(u,v))} = \left[\begin{array}{ccc}\frac{\partial x}{\partial u} & \frac{\partial y}{\partial u} & \frac{\partial z}{\partial u}\\ \frac{\partial x}{\partial v} & \frac{\partial y}{\partial v} & \frac{\partial z}{\partial v}\\ n_x & n_y & n_z\end{array}\right]^{-1}_{(u,v)}\left\{\begin{array}{c}\frac{\partial\varphi}{\partial u}\\ \frac{\partial\varphi}{\partial v}\\ \frac{\partial\varphi}{\partial n}\end{array}\right\}_{(u,v)} \tag{27}$$

However since the zero order problem is solved using the Rankine source combined of the image about the plane z=0, the first order derivatives in the free surface are computed based on Eqn. 28 in the x-direction. The y-component is computed analogously, as the second derivative in z-direction required in the first order kinematic free surface condition.

$$\frac{\partial\phi_{S_P}^{(0)}}{\partial x} = \frac{-1}{4\pi}\iint_{\partial\Omega_{-P}}\left(\phi_{S_Q}^{(0)}\frac{\partial^2 G_{PQ}}{\partial x_P\partial n_Q} - G_{PQ}\frac{\partial^2\phi_{S_Q}^{(0)}}{\partial x_P\partial n_Q}\right)d\partial\Omega_Q \tag{28}$$

The second-order derivatives in the body surface required for m-terms computation are computed following a similar procedure of Eqn. 27 considering the second order derivatives $\partial^2\phi/\partial u^2$, $\partial^2\phi/\partial v^2$, $\partial^2\phi/\partial u\partial v$, as Laplace equation to compute the spatial second order derivatives $\partial^2\phi/\partial x^2$,$\partial^2\phi/\partial y^2$,$\partial^2\phi/\partial z^2$,$\partial^2\phi/\partial x\partial y$ ... required in the m-terms computation.

Integration of the source and dipole terms

The terms regarding sources and dipoles contain singularities when the field and source points are coincident. The integral terms are given by 29 and 30, where the normal vector and Jacobian are assumed to be obtained from geometry description using NURBS. The residue of these integral were already evaluated using Green's identity assuming that no collocation points are located in the corners and the surface normal vector to be continuous in the entire geometric domain.

$$\iint_{\partial\Omega_{-P}}\varphi_Q\frac{\partial}{\partial n_Q}\left(\frac{1}{r_{PQ}}\right)d\partial\Omega_Q = PV\int_0^1\int_0^1\varphi(u,v)\frac{\partial}{\partial n}\left(\frac{1}{r_{PQ}}\right)|J(u,v)|dvdu \tag{29}$$

$$\iint_{\partial\Omega_{-P}}\frac{\partial\varphi_Q}{\partial n_Q}\frac{1}{r_{PQ}}d\partial\Omega_Q = PV\int_0^1\int_0^1\frac{\partial\varphi}{\partial n}\left(\frac{1}{r_{PQ}}\right)|J(u,v)|dvdu \tag{30}$$

The equation 29 can be discretized using the potential function approximation by B-spline, converting into 31, already taking advantage from the fact that the basis functions are null outside their influence regions to reduce the integration interval. This fact is important because it avoids the waste of numerical resources in the numerical integration procedure concerning regions where the basis function is null by construction.

$$\begin{array}{c}\int_0^1\int_0^1\varphi\frac{\partial}{\partial n}\left(\frac{1}{r_{PQ}}\right)|J(u,v)|dvdu =\\ \sum_{p=0}^{N_p}\sum_{i=0}^{N_u}\sum_{j=0}^{N_v}\phi_{i,j}^{p}\int_{u_i}^{u_{i+k_u+1}}\int_{v_j}^{v_{j+k_v+1}}N_i^{k_u,p}(u)N_j^{k_v,p}(v)\\ \frac{\partial}{\partial n}\left(\frac{1}{r_{PQ}}\right)|J(u,v)|dvdu\end{array} \tag{31}$$

The integration of source/dipole terms are performed using Gauss-Legendre quadrature for the farfield and nearfield elements as shown in Eqn. 32, where Ng_u and Ng_v are the number

[1] In the present work it was used always the same degree in both directions.

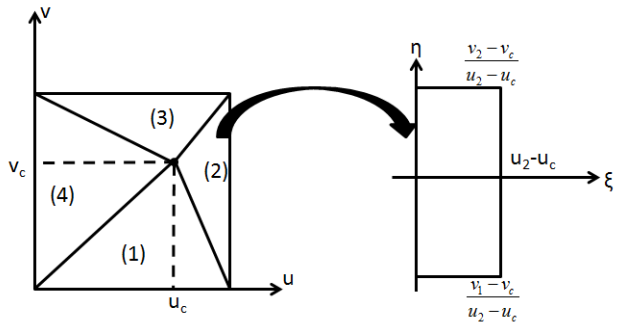

FIGURE 3. Domain splitting into 4 triangles and integration domain considering the region (2) using bi-quadratic transformation.

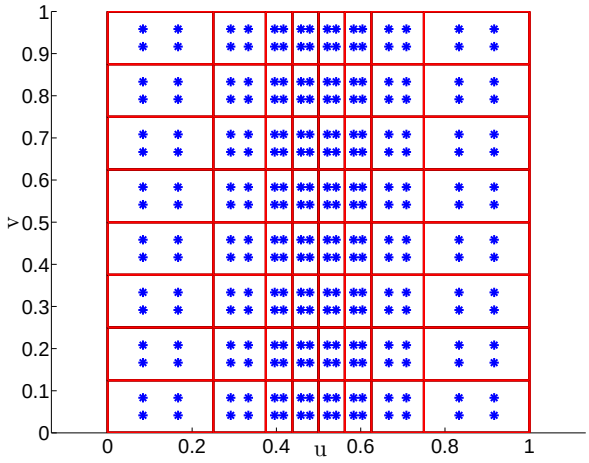

FIGURE 4. Illustration of 4 collocation points inside each panel.

of gaussian points in u and v direction, w_m and w_n are the weights and u_m and v_n are the gaussian points.

$$\int_{u_i}^{u_{i+k_u+1}} \int_{v_j}^{v_{j+k_v+1}} f(u,v)dvdu \approx \sum_{m=1}^{Ng_u} \sum_{n=1}^{Ng_v} w_m w_n f(u_m, v_n) \quad (32)$$

The self-influence terms (i.e: when the source and field points are located in the same panel) are integrated using a modification of the procedure proposed by [5] to consider the NURBS geometry description, where the panel is divided in 4 quadrilaterals, each one with a specific bi-quadratic transformation, as illustrated in Figure 3. Since this method applies the hidden layer approach regarding the potential function approximation the use of a single collocation point in each panel would lead to an undetermined linear system, providing no solution. Therefore it was assumed 4 collocation points per panel (see Figure 4) leading to an over-determined linear system, which is solved using a least-square approach, as shown in Eq. 34, where $[A]_{m,n}$ is the influence matrix, $\{c\}_{n,1}$ is the spline coefficients vector and $\{B\}_{m,1}$ is the forcing vector.

$$[A]_{m,n}\{c\}_{n,1} = \{B\}_{m,1} \quad (33)$$

$$\{c\}_{n,1} = ([A]^T_{n,m}[A]_{m,n})^{-1}[A]^T_{n,m}\{B\}_{m,1} \quad (34)$$

The free surface equations are also evaluated in terms of a least square approach since there are more equations than variables since 4 collocation panels for each panel are assumed.

Time integration

The integration in time of the ordinary differential equations is performed using a 4th order Runge-Kutta method, following the procedure described in Eqn. 39. In order to clarify the procedure, the first step is illustrated in Figure 5 and the other steps are performed analogously.

$$k_0 = f(t_i, y_i) \quad (35)$$

$$k_1 = f(t_i + 0.5\Delta t, y_i + 0.5\Delta t k_0) \quad (36)$$

$$k_2 = f(t_i + 0.5\Delta t, y_i + 0.5\Delta t k_1) \quad (37)$$

$$k_3 = f(t_i + \Delta t, y_i + \Delta t k_2) \quad (38)$$

$$y_{i+1} = y_i + \frac{\Delta t}{6}(k_0 + 2k_1 + 2k_2 + k_3) \quad (39)$$

NUMERICAL RESULTS

The study is performed for a hemisphere, a simplified geometry, in order to simplify the validation procedure. The sphere is defined by a single patch, as the free surface, which can be seen in Figure 6, assuming a 1m radius sphere with a circular free surface domain with 20m radius. In this study 11 wave periods were selected in order to provide equally spaced ka numbers between 0.4 and 1.5, where k is the wave number under 3 Froude numbers (-0.1, 0.0 and +0.1). A previous convergence analysis was performed for the null Froude number considering the slowest and highest wave period, defining the mesh 16x12 panels in the body and 30x24 panels in the free surface as the recommended one, which can be seen in Figure 7. The comparisons are performed for the zero order solution, first order forces, wave-runup and mean drift forces.

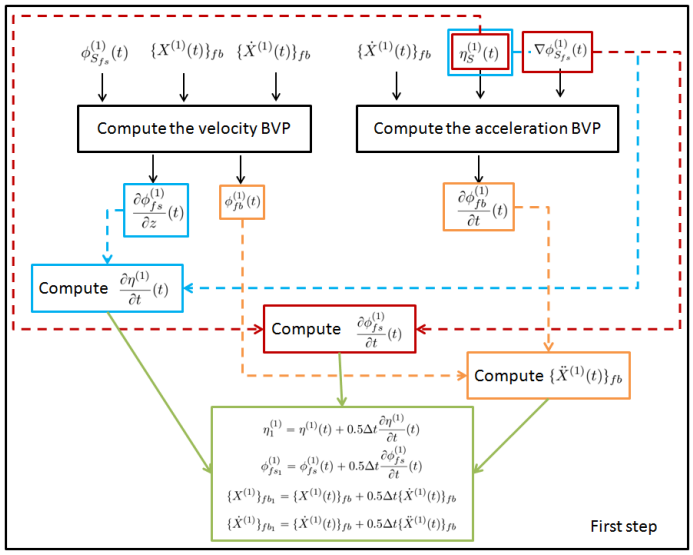

FIGURE 5. Illustration of the first step in the Runge-Kutta scheme for solving wave-body interaction.

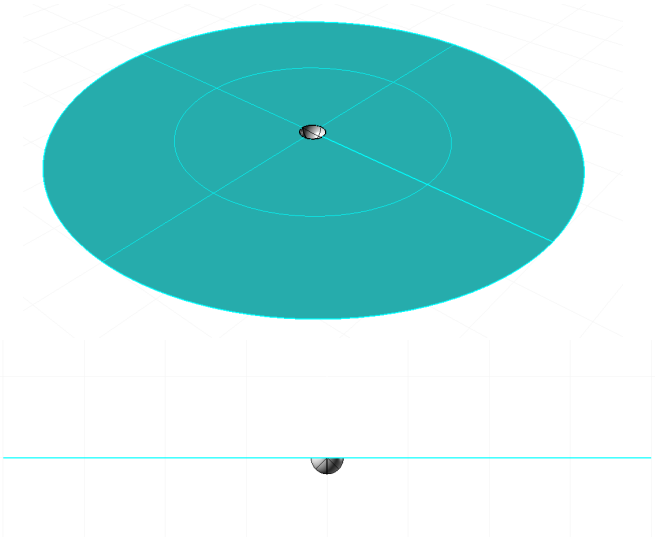

FIGURE 6. Sphere and free surface geometries.

Zero order solution

The first comparisons are performed considering the zero-order potential with the analytic solution for a unitary uniform flow. The results are compared considering the potential of order zero, flow velocity in both body surface and free surface, the last one considering the collocation points at each panel (4 points per panel). The results in the free surface, computed using the integral equation, as explained previously, can be seen from Figure 8 to 10, showing a good agreement between the numerical method and analytic solution can be verified. It should also be noticed

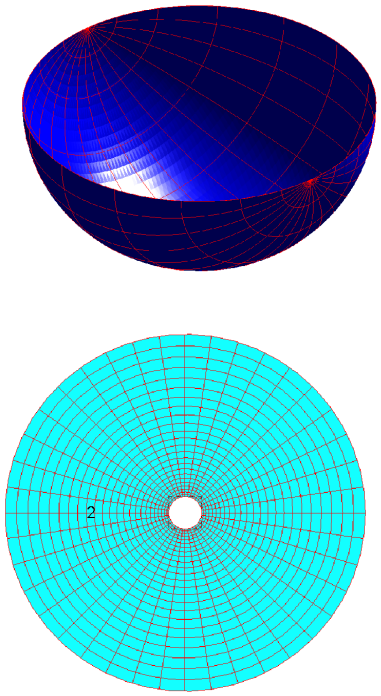

FIGURE 7. Meshes assumed in the computation of the sphere.

that due to the higher order description different points in the same panel have different velocities vectors, as verified in Figure 9 and 10. The results regarding the body surface can be verified from Figure 11 to 12, which are computed using the b-spline derivatives.

The analytical solutions for the zero order potential/derivatives can be found in several references, se for instance, [22] and are reproduced from Eqn. 40 to 43, where a is the sphere radius and U the undisturbed flow velocity magnitude.

$$\phi_S^{(0)} = -\frac{1}{2}U\frac{a^3 x}{(x^2+y^2+z^2)^{3/2}} \quad (40)$$

$$\frac{\partial\phi^{(0)}}{\partial x} = -\frac{U}{2}\left[2 - \frac{3a^3x^2}{(x^2+y^2+z^2)^{5/2}} + \frac{a^3}{(x^2+y^2+z^2)^{3/2}}\right] \quad (41)$$

$$\frac{\partial\phi^{(0)}}{\partial x} = U\frac{3a^3xy}{2(x^2+y^2+z^2)^{5/2}} \quad (42)$$

First order excitation forces

The first order excitation forces are computed in surge direction considering three Froude numbers ($F_n = V/\sqrt{ga}$): 0, 0.1 and -0.1, where the negative sign means that current and wave are in the same direction. The results are computed are compared

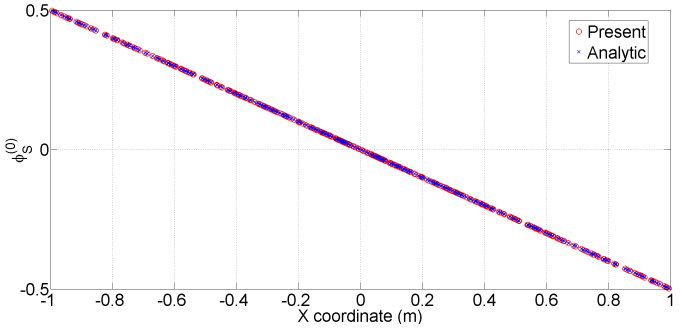

FIGURE 8. Zero order potential in the sphere surface.

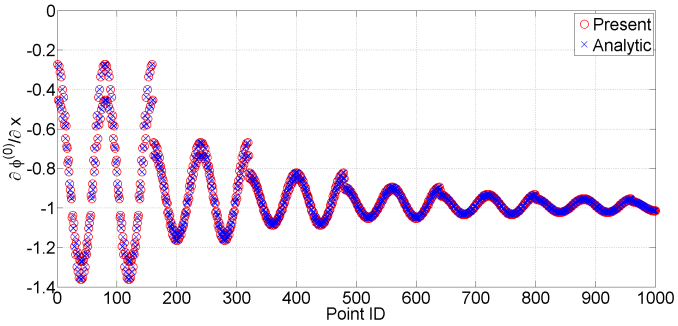

FIGURE 9. Velocity field in x direction for the zero-order potential in the free surface.

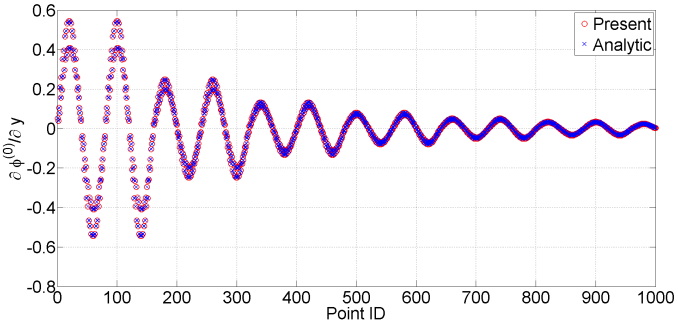

FIGURE 10. Velocity field in y direction for the zero-order potential in the free surface.

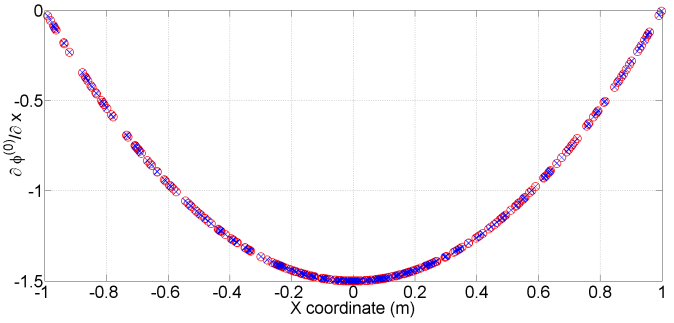

FIGURE 11. Velocity field in x direction for the zero-order potential in the body surface.

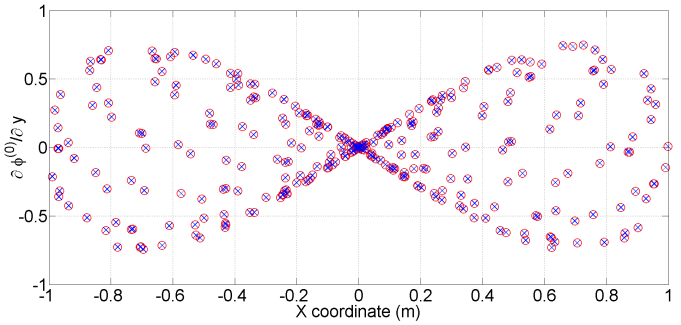

FIGURE 12. Velocity field in y direction for the zero-order potential in the body surface.

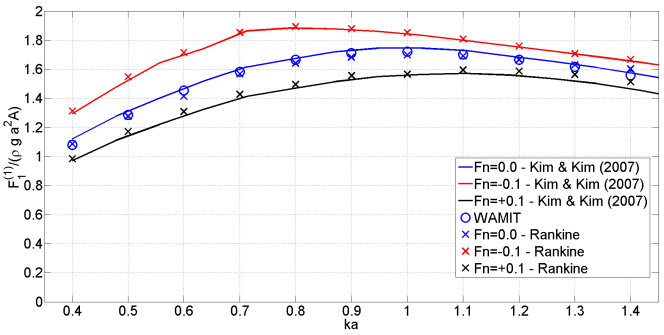

FIGURE 13. Comparison of surge first order excitation forces for a fixed sphere under several Froude numbers.

with WAMIT predictions for the zero Froude number condition and also with [10], which can be verified in Figure 13. In general a good agreement can be verified, although for the lowest and highest ka number computed there some differences. It can also be verified that the forces change appreciably in the entire ka range with large variations close to ka=0.7, where the forces considering the negative Froude are higher than the zero Froude number condition by about 20%. On the other hand for the positive Froude number condition the force is reduced 15%.

Wave runup

The comparison regarding wave runup around the fixed hemisphere is also performed and some comparisons with WAMIT results for zero Froude number are presented in Figure 14 for wave periods of 3.17s and 2.24s. It can be verified a general good agreement regarding the runup pattern for the present method and WAMIT results, although there are some differences mainly in the points located upstream for the higher frequencies. The influence of current is also evident since changes the runup pattern appreciably.

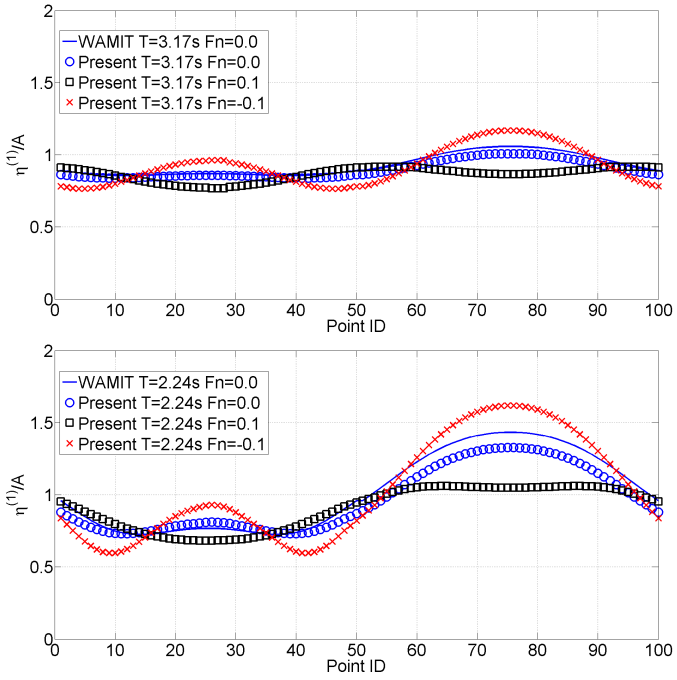

FIGURE 14. Comparison of Wave runup around the sphere for T=3.17s and T=2.24s for several Froude numbers.

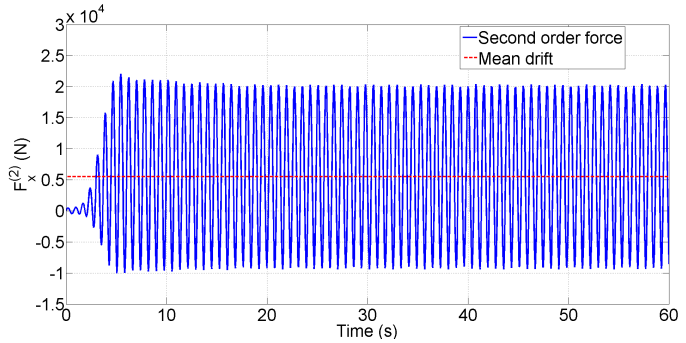

FIGURE 15. Example of the surge quadratic second order forces for a monochromatic wave for a fixed sphere ω=4 rad/s.

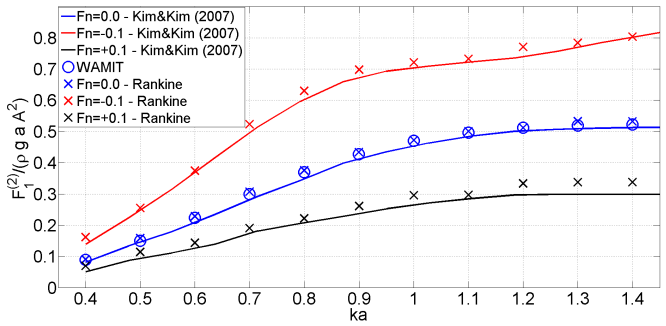

FIGURE 16. Comparison of surge mean drift forces for a fixed sphere under several Froude numbers.

Mean drift forces

The mean drift forces are computed from the second-order forces time-series using equation 43, where t_i is the transient time neglected in the mean drift forces computation to avoid the influence of transient effects in the beginning of the simulation. An example of surge second order force time series can be verified in Figure 15, where the double frequency component can also be verified in the force signal. The comparison with WAMIT prediction for the zero Froude number and the results from [10] can be verified in Figure 16, where a good agreement is verified one more time. It should be noticed that the mean drift forces change appreciably in the entire ka range and the large variations are verified close to ka=1.4.

$$\bar{F_k} = \frac{1}{\Delta t}\int_{t_i}^{t_i+\Delta t} F_k^{(2)}(t)dt,\ k = 1,2,3,...,6 \qquad (43)$$

CONCLUSIONS

This paper presented an extension of the mathematical formulation concerning the fluid-structure interaction problem in the scope of a multi-scale approach under a potential flow hypothesis to include the wave-current effects in both first and second order forces. The problems of interest requires the evaluation of the velocity field close to the body therefore the computation of the tangential derivatives of the potential function over the surfaces are important, requiring the development of a higher order panel method to overcome the limitations of the lower order one, as the free surface elevation around the hull to compute the wave run-up. The zero order problem was solved using a double flow hypothesis, providing good agreement considering the quantities in both body and free surfaces. The higher order method was developed assuming the geometry described by NURBS and the quantities in the panels by B-splines of arbitrary degree.

The zeros order velocity field was computed for a fixed hemisphere, which is essential for the computation of the wave-current interaction problem. The first order excitation forces, wave run-up and second order mean drift forces were computed and compared with WAMIT predictions for zero Froude number and the results of [10], providing a reasonable agreement concerning all quantities.

The second order mean drift forces were computed for the hemisphere providing a good agreement although for some particular points close to patch transitions or edges the velocity field and runup had some differences to WAMIT predictions, showing that the contributions due to this points to the entire forces is

negligible.

The next steps will be the comparisons for the sphere free floating condition considering results already published in frequency domain, for instance, [23]. After that, the inclusion of full second order effects will be performed considering the second order body motions and the second order problem solution.

ACKNOWLEDGMENT

The first and second authors thank FAPESP for the scholarship grants (2012/06681-7) and (2010/08778-2), respectively. Alexandre Simos acknowledges the Brazilian National Research Council, CNPq, for his research grant. Authors are wish to thank Petrobras for supporting the previous work on the low-order TDRPM code, which motivated the present development.

REFERENCES

[1] Ruggeri, F., Watai, R. A., and Simos, A. N., 2015. "A higher order time domain rankine panel method for linear and weakly non-linear computation". In Proceedings of the ASME 2015 34th International Conference on Ocean, Offshore and Arctic Engineering. DOI:10.1115/OMAE2015-42234.

[2] Piegl, L., and Tiller, W., 1997. *The NURBS Book*, second ed. Springer Verlap Berlin.

[3] Ruggeri, F., 2012. A time domain rankine panel method for 2d seakeeping analysis. MSc. Thesis - University of Sao Paulo.

[4] Watai, R. A., 2014. "A time-domain boundary elements method for the seakeeping analysis of offshore systems". PhD thesis, University of Sao Paulo.

[5] Maniar, H. D., 1995. "A three dimensional higher order panel method based on b-splines". PhD thesis, MIT - Massachusset Institute of Technology.

[6] Liu, Y. H., Kim, C. H., and Lu, X. S., 1991. "Comparison of higher-order boundary element and constant panel methods for hydrodynamic loadings". *International Journal of Offhsore and Polar Engineering,* ***1***(1).

[7] Camas, B. S., 2015. "A time-domain finite element method for seakeeping and wave resistance problems.". PhD thesis, Universidad Politcnica de Madrid (UPM).

[8] Lee, C.-H., and Newman, J. N., 2005. *Numerical Models in Fluid-Structure Interaction*. WIT Press, ch. Computation of wave effects using the panel method, pp. 211–251.

[9] ANSYS, 2009. *AQWA LINE MANUAL - Release 12.0*, April.

[10] Kim, D. J., and Kim, M. H., 1997. "Wave-current interaction with a large three-dimensional body by thobem". *Journal of Ship Research,* ***41***(4), pp. 273–285.

[11] Shao, Y.-L., 2010. "Numerical potential-flow studies on weakly-nonlinear wave-body interactions with/without small forward speeds". PhD thesis, NTNU - Norwegian University of Science and Technology.

[12] Maniar, H., 1995. "A b-spline based higher order method in 3d". In 10th Workshop on Water Waves and Floating Bodies.

[13] Timman, R., and Newman, J. N., 1962. The coupled damping coefficients of a symmetric ship. Tech. rep., Hydromechanics Laboratory.

[14] Nakos, D. E., Kring, D. C., and Sclavounos, P. D., 1993. "Rankine panel methods for transient free surface flows". *6th International Conference on Numerical Ship Hydrodynamics*.

[15] Van't Veer, A. P., 1998. "Behavior of catamarans in waves". PhD thesis, TU Delft.

[16] Wehausen, J. V., and Laitone, E. V., 1960. *Surface Waves*. SpringerVerlag.

[17] Cummins, W. E., 1962. The impulse response function and ship motions. Tech. Rep. 1661, David Taylor Model Basin, October.

[18] Israeli, M., and Orszag, S. A., 1981. "Approximation of radiation boundary conditions". *Journal of Computational Physics*.

[19] van Daalen, E. F. G., 1993. "Numerical and theoretical studies of water waves and floating bodies". PhD thesis, University of Twente.

[20] Tanizawa, K., 2000. "The state of the art on numerical wave tank". In Proceeding of 4th Osaka Coloquium on Seakeeping Performance of Ships, pp. 99–114.

[21] Bandyk, P. J., and Beck, R. F., 2011. "The acceleration potential in fluid-body interaction problems". *Journal of Engineering Mathematics,* ***70***, pp. 147–163. DOI: 10.1007/s10665-010-9446-0.

[22] Milne-Thomson, L. M., 1968. *Theoretical Hydrodynamics*. Dover Publications Inc.

[23] Huijsmans, R. H. M., 1996. "Mathematical modeling of the mean wave drift force in current : A numerical and experimental study". PhD thesis, TU Delft.